Joint Scholte-wave and diving-wave FWI

L. Letki[1], M. Ramzy[1], K.C. Goh[1], J. McLeman[1], G. Hampson[1], T. Rayment[1], G. Cambois[2], T. Alkatheeri[2]

[1] DUG Technology; [2] ADNOC

Summary

In this paper, we demonstrate that Scholte waves, often considered a source of noise in ultra-shallow water environments, can be effectively exploited as valuable signal when jointly inverted with diving waves using full-waveform inversion (FWI). By carefully analysing the recorded wavefield and adopting a staged elastic FWI strategy, we successfully resolve the near-surface kinematics in a challenging hard-seabed setting where conventional acoustic DW-FWI would be unreliable. The joint use of surface and diving waves enables robust updates of both P-velocity and the ratio of S-velocity over P-velocity in the very shallow subsurface, providing a reliable starting point for deeper model updates. The improved data fit, excellent well correlations, and geologically consistent models confirm that this approach delivers a high-fidelity near-surface model, ultimately enabling reliable imaging of deeper targets.

Joint Scholte-wave and diving-wave FWI

Motivation

In seismic imaging, accurately resolving near-surface kinematics is essential for velocity estimation at depth, correct depth positioning of geological layers, and ultimately reliable target identification. In shallow-water environments, full-waveform inversion (FWI) has become the industry standard, overcoming the limitations of reflection tomography due to the restricted illumination angles of shallow reflections by using diving waves recorded over a wide range of offsets. Diving-wave FWI (DW-FWI) updates the P-wave velocity (V_p) within the subsurface region illuminated by these diving waves; however, the depth of penetration depends not only on the maximum recorded offset but also on the geological setting, with strong velocity contrasts limiting penetration and creating shadow zones.

In ultra-shallow water, additional challenges arise. Air-gun size limitations result in a relative lack of low frequencies, typically required to mitigate cycle skipping. Furthermore, strong elastic effects occur at the water–bottom interface, leading to the generation of surface waves known as Scholte waves. In the presence of a hard seabed, these Scholte waves can exhibit amplitudes significantly higher than those of the low-frequency diving waves. Their interference can therefore compromise the reliability of DW-FWI, making near-surface kinematic resolution particularly challenging. In this paper, we demonstrate how Scholte waves, used in combination with diving waves, can be exploited to resolve shallow kinematics in a case study from an ultra-shallow-water environment (5–30 m) with a hard, rugose seabed. The dataset considered consists of the deblended hydrophone component of an ocean-bottom node (OBN) survey.

Method: understand the recorded wavefield to build a strategy

To design an effective imaging strategy, it is essential to understand the different components of the recorded wavefield and how each contributes information toward building an accurate subsurface model.

At low frequencies (below 9 Hz), the recorded signal is dominated by Scholte waves. From a kinematic perspective, these surface waves carry information on both V_p and S-wave velocity (V_s) in the very near surface. In non-homogeneous media, these Scholte waves are dispersive, with their depth of penetration decreasing with increasing frequency. Using the full elastic wave equation, we modelled these waves at different frequencies from 4 to 16 Hz. The modelling experiments allow visualisation of the particle motion as the surface waves propagate along the seabed (Figure 1), confirming the accurate simulation of the associated pressure wavefield. It is also used to estimate the depth of penetration at the considered frequency.

Diving P-waves are recorded across the seismic bandwidth, and their kinematics strongly depend on the P-wave velocity. To assess their depth of penetration, wave-equation–based illumination analysis was performed, accounting for both source- and receiver-side effects across a range of maximum offsets (Figure 2). This analysis forms the basis of an offset-stepping strategy for DW-FWI, in which the shallow part of the model is updated first to reduce the risk of cycle skipping.

Elastic effects influence not only the amplitude of diving waves but also their phase. While amplitude errors introduced by acoustic modelling can be partially mitigated through normalisation during DW-FWI, phase distortions directly affect the apparent kinematics. Accurate modelling of diving-wave kinematics, therefore, requires the elastic wave equation and a reliable near-surface V_s model, which is linked to the correct simulation of surface waves.

At higher frequencies (12 Hz and above), the surface-wave energy diminishes, and the diving waves can provide detailed updates of the P-velocity within their zone of illumination. Below the depth of diving-wave penetration, deeper reflections and their multiples are used to jointly invert for velocity and impedance using multi-parameter FWI (MP-FWI), thereby honouring both the kinematic and dynamic aspects of the recorded data. In an elastic MP-FWI framework (McLeman et al., 2023), this approach enables the inversion of elastic parameters: V_p, P-impedance, and V_s/V_p ratio.

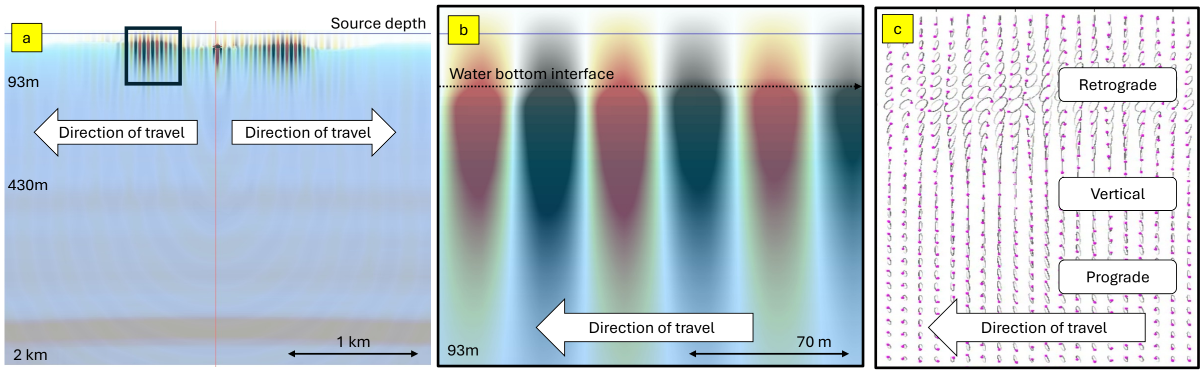

Figure 1 *Surface waves modelling: snapshot of the wavefield modelled through the initial model as a reciprocal experiment using the elastic wave equation and a source wavelet with a narrow bandwidth around 8 Hz. (a) The pressure wavefield overlaid on the initial* V_p *model shows weak diving waves and strong surface waves. The zoom on the surface waves pressure wavefield (b) shows a depth of penetration beyond 100 m below the seabed. (c) A representation of the particle trajectory, as the surface waves travel, highlights the expected changes with depth, from retrograde motion to vertical and then prograde motion deeper down (Zhao et al., 2022).*

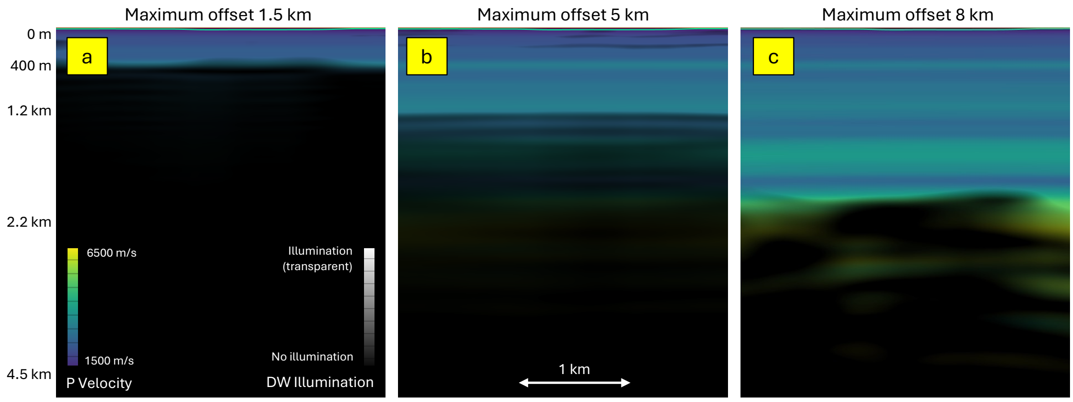

Figure 2 *Overlay of the initial P velocity model with modelled diving wave illumination volume (crossline view) for a maximum offset of 1.5 km (a), 5km (b) and 8 km (c).*

Based on the analysis of the recorded wavefield, the following inversion strategy was developed:

- Starting at 6 Hz, a joint full-elastic FWI of Scholte waves and diving waves is performed to simultaneously update V_p and V_s/V_p ratio in the very near-surface.
- Between 12 and 30 Hz, limited-offset DW-FWI is applied to refine the near-surface V_p model.
- This is subsequently extended to a long-offset 12 Hz DW-FWI, allowing the V_p model to be updated down to the maximum depth of diving-wave penetration.
- With a well-resolved shallow kinematic model in place, the shallow P-impedance is updated using reflections, including their ghosts and multiples. At these short offsets, no additional kinematic information is extracted from the reflections.
- Finally, both kinematics and dynamics in the deeper part of the model are updated through a joint multi-parameter FWI (MP-FWI) of V_p and P-impedance, incorporating deeper reflections as well as free-surface and interbed multiples. This step pushes kinematic updates to deeper targets and provides a robust starting point for higher-frequency elastic MP-FWI, jointly inverting for elastic properties V_p, P-impedance and V_s/V_p ratio.

Results

To evaluate the inversion results, several levels of quality control (QC) are analysed. The first-level QCs assess whether the inversion has achieved its primary objective, namely improving the agreement between the observed and modelled data. As shown in Figure 3a, after the joint surface-wave and diving-wave (SW & DW) FWI update, the modelled data closely reproduce the observed surface and diving waves. The corresponding FK spectrum demonstrates that the dispersive behaviour of the surface waves is accurately captured by the updated model. Figures 3b and 3c further illustrate the consistency between modelled and observed diving waves following DW-FWI using progressively longer offsets, successfully reproducing the wavefield patterns associated with the strong velocity contrasts and resulting shadow zones.

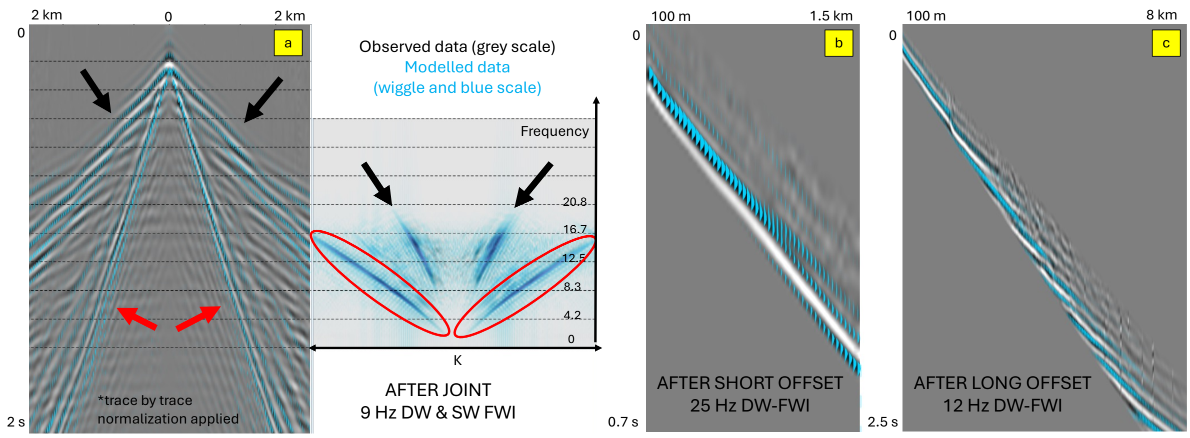

Figure 3 *Overlay of observed and modelled example receiver gathers: (a) after joint SW & DW FWI, with overlay of associated FK spectra - the surface waves are highlighted in red, diving waves in black - (b) after short offset DW-FWI up to 25 Hz and (c) after long offset DW-FWI up to 12 Hz.*

The second-level QC verifies that the updated models are consistent with all available data. As illustrated in Figure 4, the well correlation demonstrates an excellent match between the well profiles for both V_p and V_s/V_p following the resolution of near-surface kinematics using joint SW & DW FWI, followed by DW-FWI. Elastic MP-FWI is expected to further enhance the resolution of these models.

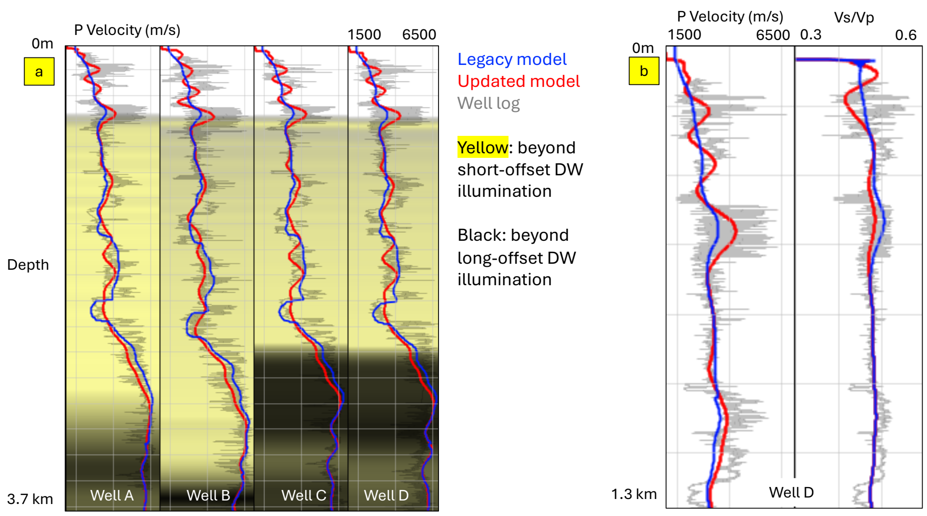

Figure 4 *(a) Overlay of well logs with curves extracted from the legacy V_p model and from the V_p model updated using joint SW & DW-FWI, followed by short-offset and long-offset DW-FWI, with DW illumination limits overlaid in yellow (short-offset) and black (long-offset). (b) Zoom on the shallow well correlation for well D, highlighting the shallow details captured on both the updated V_p and V_s/V_p model.*

Finally, the third-level QC takes a more interpretative approach by assessing whether the updated models are geologically plausible. Figure 5 presents an overlay of the V_p and V_s/V_p models with the inverted shallow reflectivity obtained using MP-FWI, from the field data, including reflections, ghosts, and multiples. The level of detail in the shallow reflectivity is particularly notable, as these depths are typically poorly imaged by conventional methods due to limited illumination.

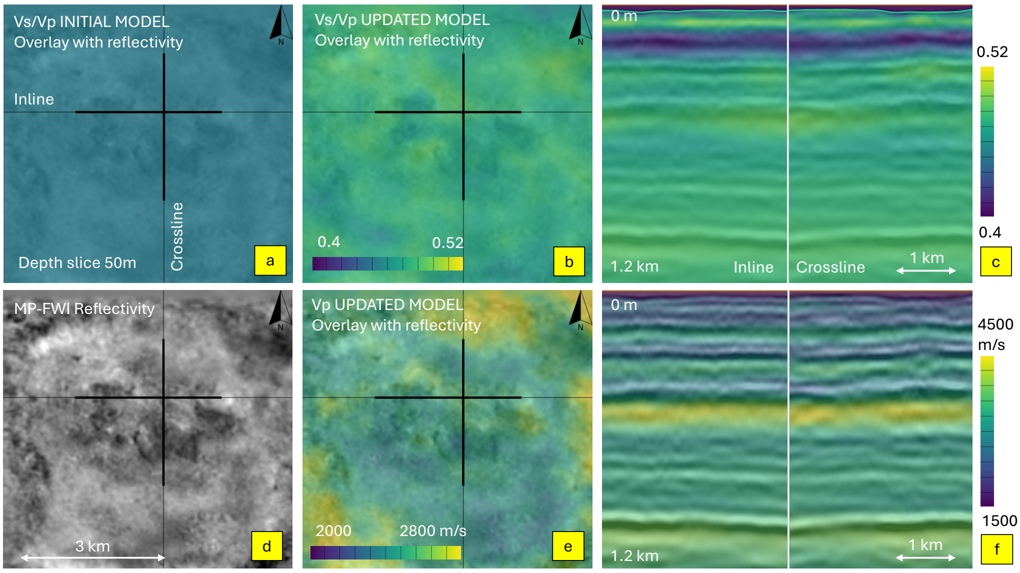

Figure 5*(a) Depth slice through the initial V_s/V_p model, (b) updated V_s/V_p model and (c) inline/crossline through the updated V_s/V_p model. All models are overlaid with the shallow reflectivity obtained using MP-FWI. (d) Depth slice through the reflectivity model. (e) Depth slice through the updated V_p model and (f) corresponding inline/crossline highlighting the geologically consistent shallow details.*

Conclusions

In this study, we demonstrate that Scholte waves, often considered a source of noise in ultra-shallow water environments, can be effectively exploited as valuable signal when jointly inverted with diving waves. By carefully analysing the recorded wavefield and adopting a staged elastic FWI strategy, we successfully resolve the near-surface kinematics in a challenging hard-seabed setting where conventional acoustic DW-FWI would be unreliable. The joint use of surface and diving waves enables robust updates of both V_p and V_s/V_p in the very shallow subsurface, providing a reliable starting point for deeper model updates. The improved data fit, excellent well correlations, and geologically consistent models confirm that this approach delivers a high-fidelity near-surface model, ultimately enabling reliable imaging of deeper targets.

Acknowledgements

The authors wish to thank ADNOC and DUG Technology for permission to publish these results.

References

McLeman, J., Rayment, T., Burgess, T., Dancer, K., Hampson, G. and Pauli, A. [2023] Superior resolution through multiparameter FWI imaging: A new philosophy in seismic processing and imaging. *The Leading Edge*, **42**(1), 34-43.

Zhao, S., Meng, X., Gu, D., Guo, C., Wang, X. and Zhang, J. [2022] Study on propagation characteristics of Scholte wave in shallow sea at non-horizontal underwater interface, *Journal of Vibroengineering*, **24**(3), 521-536.